High precision photometry: detection of exoplanet transits using a small telescope

Darryl Sergison

The successful detection and measurement is reported of milli-magnitude scale lightcurve dips caused by the transits of known exoplanets in front of their parent stars. Data have been obtained using a small aperture (0.25m) telescope from Gothers Observatory, a non-optimal sea level coastal location in Cornwall, UK. Observations of five transiting systems, HAT-P-9b, HAT-P-13b, TrES-1b, TrES-3b and Gliese 436b indicate that transit studies with a precision of better than ±4mmag are regularly achievable and that useful transit timing and depth measurements may be made.

Introduction

The discovery of planets orbiting other stars has to rank as one of the most significant scientific discoveries in modern times. In many ways it confirms strongly suspected ideas that planetary systems are common, however now we have the data to support the conclusion that we live in just one of a plethora of systems scattered through our part of the Milky Way galaxy.

As of 2012 May 12, 612 exoplanet candidates have been discovered[1] and as with many other fields in astronomy, opportunities exist for amateurs to make valuable contributions to their study. The mechanism described here is via the transit method, which makes use of fortuitous circumstances where the orbital plane of a planetary system is coincident with the line of sight of observers on Earth.[2]

Under these circumstances, the star is seen periodically to dim as the planetary companion transits the disc of the star, temporarily blocking some of the observed stellar flux. Typically transit dips amount to less than 20 milli-magnitudes and as a result place exacting requirements on controlling the noise that is inevitably present in the photometric measurement.

This paper describes observations made with fairly modest equipment that yield scientifically useful high precision data and contribute to long term studies of known transiting exoplanet systems.

Objectives and scientific value

Observations of known transiting exoplanets are of particular interest as they allow accurate long term monitoring of any transit timing variations. This can offer information on orbital decay or evolution of closely orbiting planets. It is also a powerful tool to detect anomalies in mid-transit times caused by the gravitational influence of another undetected body in the planetary system.[3]

Equipment

Observations of exoplanet transits were made at the author's small home observatory in Gothers, St Dennis, Cornwall using a 0.25m Meade LX200 Schmidt–Cassegrain telescope on an EQ6 German Equatorial mount (Figure 1). In order to minimise zero-point errors, targets were chosen which did not require a meridian flip during the transit or for a period of 1 hour before ingress or after egress. The optical system is equipped with a focal reducer to yield a focal ratio f/6.8 and a focal length of approximately 1700mm.

The CCD imager is the QHY6 Pro device, featuring a 752×585 array of 8.6×8.3micron pixels. The CCD is operated using set point cooling at temperatures between −12 and −15°C. All observations were taken un-binned, yielding an image scale for all but the first dataset of 1.01"×0.98" per pixel. Images were bias, dark and flat field corrected and no other image enhancements were made.

Autoguiding is helpful in reducing noise generated by spatially imperfect flat field correction.

Figure 1. The telescope used to collect the data presented in this paper. 0.25m SCT with 0.1m refractor guidescope, mounted on an EQ6 in a simple roll-off-roof observatory.

Autoguiding was performed using a QHY5 CMOS detector and the free guiding software package 'PhD'.[4] A separate 100mm diameter, 600mm focal length refractor guidescope was used, and great care was taken to minimise differential flexure through the structure.

Methods

A time-series of the selected targets was taken with an exposure time and cadence that depended on the brightness of the objects under study. Basic data on the objects reported in this paper may be found in Table 1.

Exposure times were chosen so that the maximum ADU (analog/digital unit) count remained within the linear portion of the CCD response; this corresponds to a value of less than 40,000 ADU for the CCD used. For the brightest targets this can result in a very short exposure time (a few seconds), which introduces an unacceptable component of scintillation noise on such a small aperture. As a result, strategies such as filtering and defocus were used to limit the maximum ADU count and increase exposure times to a few tens of seconds.

For the brighter objects (V<11) any of the standard Johnson/Cousins V, R, and I photometric bands may be used as the signal-to-noise ratio (SNR) is high even with a large proportion of the spectrum rejected. For fainter objects it is possible to image unfiltered although this can lead to problems due to differential extinction between the target and reference star if their colour indices are significantly different. This leads to a strong baseline curvature on the lightcurve.

While it is possible to model and remove the baseline curvature, a better solution is to use a long-pass filter such as the Kodak Wratten 12, which is inexpensive (less than £10) and easily available (the filter transmission characteristics are shown in Figure 2). The use of this filter minimises differential extinction issues and maximises SNR on the object within reasonable exposure cadence. The root of the differential extinction problem lies in the fact t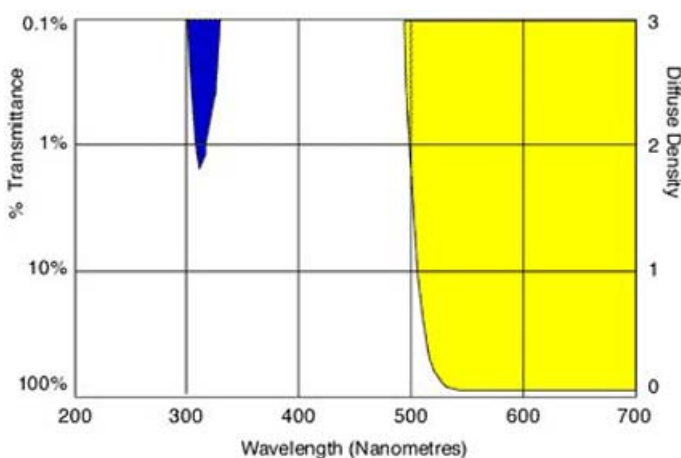hat atmospheric extinction is stronger at the blue end of the spectrum than the red. As observations progress through the night, a blue star will experience a greater variation in magnitude as a function of airmass than a red star. As a result, unless your target and reference stars are of identical colour (which is rare) the differential extinction will cause the baseline magnitude of the target star to appear to change as a function of airmass. The use of a filter that removes much of the blue end of the spectrum (such as the Wratten 12) reduces this effect.

Reduction was performed using standard differential aperture photometry techniques. Comparison stars are selected that are as close as possible in angular separation, colour and brightness to the target. The angular separation should be small, partly as the author owns a small CCD sensor and partly so that transparency variations (such as thin cirrus cloud) are minimised between the target and comparison stars. Brightness differences should also be minimised where possible so that a high SNR may be achieved on both the target and comparison stars, while preventing either from entering the non-linear part of the CCD response.

It is important when undertaking high precision photometry to optimise the measurement aperture of the star image being measured. As the target and reference stars are generally bright, high-SNR objects, it is important to ensure that the measurement aperture is not too small. In particular, variations in seeing will change the diameter of the star's point spread function (PSF) and cause small changes in the proportion of the PSF that falls outside of the measurement aperture. While these changes in measured PSF fraction are small and would not compromise asteroid or variable star photometry, the small variations that are being measured in an exoplanet transit make this effect important.

Typically sky conditions during observations were clear but not always photometric. Airmass was always less than 2: hence observations made at altitudes of greater than 30°.

Photometry was performed using Maxim DL[5] and data manipulation using Microsoft Excel.

Model fitting was performed using the transit-fitting tool on the Exoplanet Transit Database (ETD) provided by the variable star section of the Czech Astronomical Society.[6] This is a very useful website which provides a variety of services for the exoplanet observer, including a shared repository for observations.

The ETD tool allows the user to fit their data using a least squares fit to models generated for each transit based on previously measured parameters. Free parameters available for fit optimisation include transit duration, mid-transit time and transit depth. The tool returns the best fitted lightcurve and derived system properties such as measured orbital inclination.[7] It also provides an estimate of residuals and a 'quality' factor that incorporates measurement precision and sampling cadence.
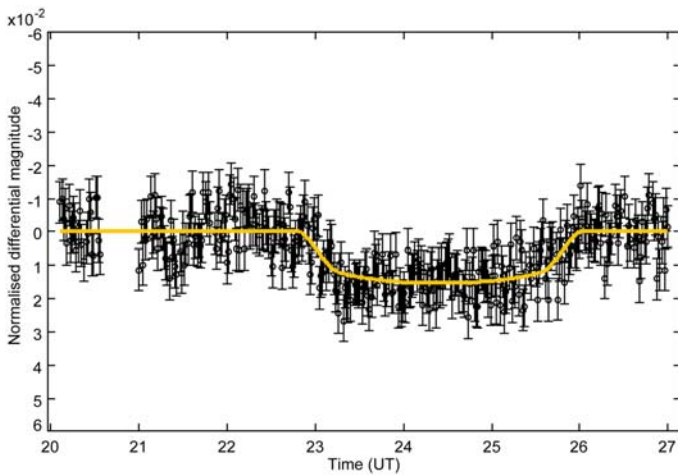
Table 1. Target exoplanet system characteristics

(data from http://var2.astro.cz/ETD/index.php)

Exoplanet system	RA hh mm ss	Dec dd mm ss	V mag	Predicted transit depth (mag)	Predicted transit duration (min.)
HAT-P-9b	07 20 40.5	+37 08 26	12.3	0.0126	206
HAT-P-13b	08 39 31.8	+47 21 07	10.6	0.0065	193.7
GJ 436b	11 42 10.0	+26 42 37	10.7	0.009	62
TrES-3b	17 52 07.0	+37 32 46	12.4	0.0291	77.4
TrES-1b	19 04 09.8	+36 37 58	11.8	0.0208	149.8

Figure 2. An ideal exoplanet transit filter for small telescopes – the Kodak Wratten 12. This diagram shows the fraction of light transmitted by the filter, indicating that transmission is almost 100% above 500nm and almost 0% below 500nm. The small light leak in the near ultraviolet is insignificant especially since the atmosphere is relatively opaque in this region of the spectrum.

Figure 3. Lightcurve of HAT-P-9b transit on 2010:12:24. Transit depth is 15.7±1.1mmag. Transit duration is 194±5 minutes.
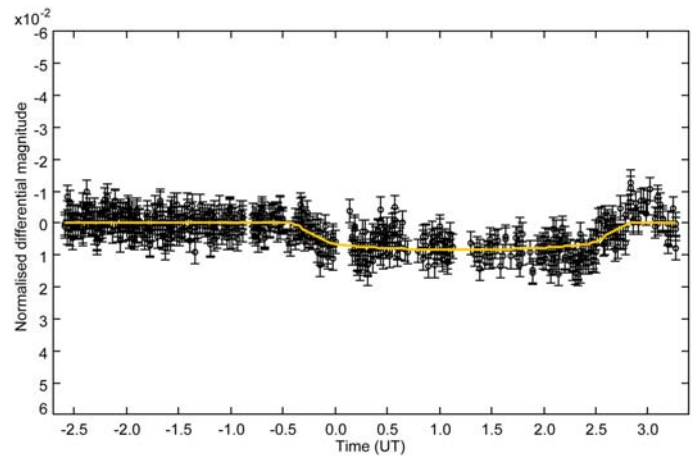

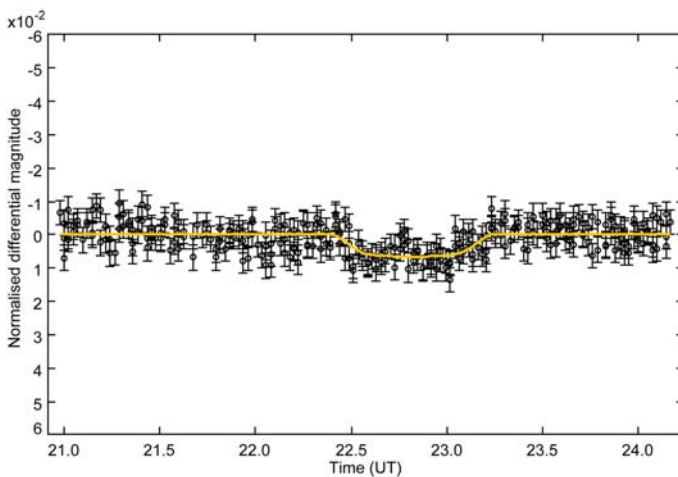**Figure 4.** HAT-P-13b transit lightcurve on 2011:03:06. Transit depth is 8.7±0.5mmag. Transit duration is 201±4 min.

Figure 5. Lightcurve of GJ 346b on 2011:03:12. Transit depth is 7.0±0.6mmag. Duration is 52±3 min.
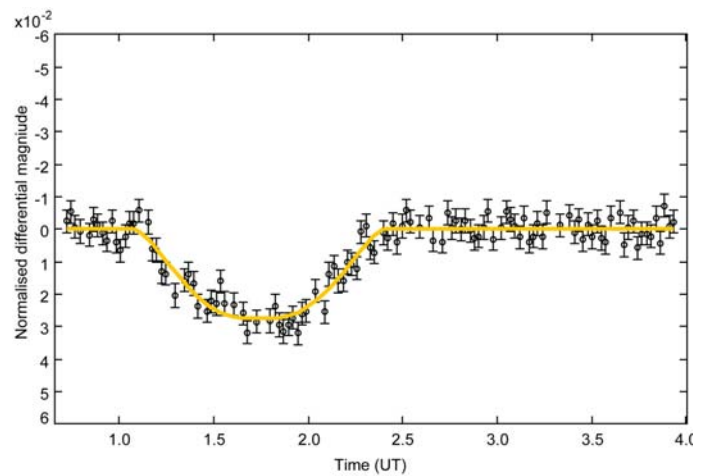

Figure 6. Lightcurve of TrES-3b on 2011:04:26. Transit depth is 27.9±1.2mmag. Duration is 80.8±2.4 min.

Observing details and photometric accuracy

An analytical assessment of the uncertainties in the photometry is difficult as there are many varied parameters that drive the noise on the signal observed. Thus an estimation of the photometric uncertainties was performed through calculation of standard deviation from the ETD-modelled fit. This method does leave the data subject to uncertainties on the part of the model, however the author feels that this is small compared to that on the photometry.

Table 2 lists summarised data of each observing run and associated photometric uncertainties. Details of comparison stars and all raw data may be accessed via the ETD using the observation reference listed.

The best results using the system described above gave 1-sigma standard deviation values of less than 4 milli-magnitudes on three occasions and ~2mmag on one occasion. These were on individual

frames without any averaging or stacking applied.

The author feels that while they are already close to the limit in terms of performance, some further optimisation of equipment and imaging strategy could see residuals fall reliably below 2mmag.

Results

The lightcurves of measured transit photometry are presented in Figures 3 to 8. The Figures show individual photometric measure-

Table 2. Image parameters and error measurements

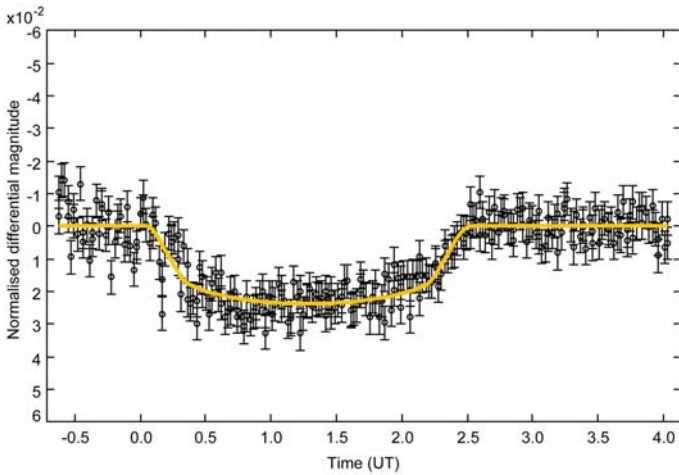|	HAT-P-9b	HAT-P-13b	GJ 436b	TrES-3b	GJ 436b	TrES-1b
Date	2010:12:24	2011:03:06	2011:03:12	2011:04:26	2011:04:27	2011:04:28
Filter	Wratten25A	Wratten 12	Johnson V	Wratten 12	Wratten 12	Wratten 12
Exposure time (sec)	60	12	30	90	60	60
Mag (Johnson V)	12.3	10.62	10.68	12.4	10.68	11.79
Photometric aperture diameter (pixels)	8	8	12	14	16	16
CCD temp (°C)	−15	−15	−15	−12	−12	−12
Focal length (mm)	1450	1700	1700	1700	1700	1700
FWHM (arcsec)	3.5	4.2	4.3	4.6	9.9 (defocused)	4.7
Standard deviation on individual frames (mmag)	6.3	3.7	3.7	3.5	1.7	5.0

Figure 7. Lightcurve of TrES-1b on 2011:04:28. Transit depth is 24.1±1.2mmag. Transit duration is 148.2±2.4 min.
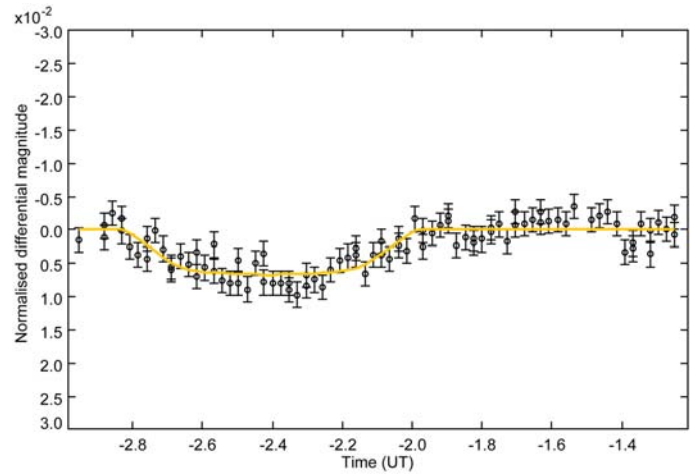

Figure 8. Lightcurve of GJ 436-b on 2011:04:27. Transit depth is 6.8±0.7mmag. Duration is 52±2 min.

Table 3. Predicted and measured parameters of exoplanet transits observed from Gothers Observatory

Transit	Date	Predicted duration (mins)	Measured duration (mins)	Predicted depth (mmag)	Measured depth (mmag)
HAT-P-9b	2010:12:24	206	194±5	12.6	15.7±1.0
HAT-P-13b	2011:03:06	193.7	201±4	6.5	8.7±0.5
GJ 436b	2011:03:12	62	52±3	9.0	7.0±0.6
TrES-3b	2011:04:26	77.4	80.8±2.4	29.1	27.9±1.2
GJ 436b	2011:04:27	62	52±2	9.0	6.8±0.7
TrES-1b	2011:04:28	149.8	148±2.4	20.8	24.1±1.2

ments as a function of time through the predicted transit period. Photometry is normalised to zero for the out-of-transit magnitude. Error bars on the averaged points are of 1 standard deviation from the model fit. The solid yellow line is the fitted model transit found using the ETD tool. Residual baseline curvature is removed using a second order polynomial fit via the ETD tool.

All plots except the last are scaled to the same Y-axes to illustrate the relative transit depths and measurement uncertainties. The last plot GJ436b is of sufficiently high precision that the axes are doubled in scale to better show the shallow transit.

A summary of the transit parameters, compared with predictions based on previously calculated ephemeris data, is seen in Table 3.

Conclusions

This paper reports transit observations for the five extrasolar planets: HAT-P-9b, HAT-P-13b, TrES-1b, TrES-3b and GJ 436b. The use of the model-fitting tool provided by the variable star section of the Czech Astronomical Society allows geometric transit parameters to be calculated from the fitted transit data. These parameters are given in Table 4.

It may be noted that most of the planets studied are slightly larger than Jupiter, with the exception of GJ 436b, a 'hot Neptune-sized' planet orbiting an M-dwarf star in Leo.[8] Without exception, all of the planets stud-

ied are in short period orbits, much closer to their parent star than any planets within our own solar system.

Observations reported here demonstrate that telescopes of modest aperture, equipped with relatively low-cost CCD cameras and situated in less than optimal locations, can be used to obtain usefully accurate data on exoplanets transiting stars of 12th magnitude and brighter. These observations are valuable in that they can be incorporated in a worldwide database and used to monitor long-term variations in planetary system behaviour.

Address: 5 Gothers Road, St Dennis, Cornwall PL26 8DF. [darryl_sergison@hotmail.com]

References

1 http://exoplanet.eu/catalog-all.php
2 Winn J. N., 'Exoplanet transits and occultations', in *Exoplanets*, *ed.* Seager S., University of Arizona Press, 55–77 (2010)
3 Nascimbeni V. *et al.*, 'TASTE II: A new observational study of transit time variations in HAT-P-13b', *Astron. Astrophys.* 532, A24 (2011)
4 Stark C., PhD guiding software, **http://www.stark-labs.com/phd guiding.html**
5 Maxim DL, Image processing software by Diffraction Ltd, **http://www. cyanogen.com/maxim_main.php**
6 Brat L., Exoplanet Transit Database, **http://var2.astro.cz/ETD/ protocol.php**
7 Pejcha O., Exoplanet transit parameters from amateur astronomers' observations, **http://var2.astro.cz/ETD/FitProcedureDescription-Pejcha2008.pdf** (2008)
8 Bean J. L. *et al.*, 'A Hubble Space Telescope transit light curve for GJ 436b', *Astron. Astrophys.* 486, 1039–1046 (2008)

Table 4. Derived system geometries for exoplanets studied

Planet	Measured planetary radius (Jupiter radii)	Catalogue planetary radius (Jupiter radii)	Measured orbital inclination (°)	Catalogue orbital inclination (°)
HAT-P-9b	$1.52_{-0.06}^{+0.05}$	1.40±0.06	$85.7_{-1.3}^{+1.6}$	86.50±0.20
HAT-P-13b	$1.36_{-0.05}^{+0.05}$	1.28±0.08	$83.6_{1.6}^{+1.8}$	83.30±0.62
GJ 436b (Obs. 1)	$0.36_{-0.02}^{+0.02}$	0.44±0.04	$86.0_{-0.3}^{+0.4}$	85.80±0.25
TrES-3b	$1.26_{-0.03}^{+0.03}$	1.31±0.09	$81.9_{-1.6}^{+1.7}$	82.15±0.21
GJ 436b (Obs. 2)	$0.36_{-0.02}^{+0.02}$	0.44±0.04	$86.1_{-0.4}^{+0.4}$	85.80±0.25
TrES-1b	$1.18_{-0.03}^{+0.03}$	1.08±0.03	$88.1_{-1.0}^{+1.9}$	88.40±0.30